Journal of Thermal Analysis and Calorimetry, Vol. 96 (2009) 2, 463–468

PHASE TRANSITION IN LAMOX TYPE COMPOUNDS

*M. Ali (Basu), B. N. Wani and S. R. Bharadwaj**

Chemistry Division, Bhabha Atomic Research Centre, Trombay, Mumbai 400 085, India

$La_2Mo_2O_9$ (LMO) was synthesized at lower temperature 973 K (LT-phase) by ceramic route. Differential thermal analysis (DTA) scan of LT-phase of LMO showed $\alpha \rightarrow \beta$ transition at 843 K during heating and $\beta \rightarrow \alpha$ conversion via a metastable γ-phase during cooling. This was also confirmed by thermo-dilatometry and impedance spectroscopy. $La_2Mo_{1.95}V_{0.05}O_{9-\delta}$ (LMVO), $La_{1.96}Sr_{0.04}Mo_2O_{9-\delta}$ (LSMO) and $La_{1.96}Sr_{0.04}Mo_{1.95}V_{0.05}O_{9-\delta}$ (LSMVO) were prepared in a similar way. These compounds exhibited $\alpha \rightarrow \beta$ transition on heating with shift in transition temperature, but the existence of γ-phase during cooling disappeared. Substitution increased the ionic conductivity of α-phase and reduced that of β-phase.

Keywords: *dilatometry, electrical conductivity, $La_2Mo_2O_9$, Phase transition, X-ray diffraction*

Introduction

Ionic conductors with high conductivity of oxygen ions have been attracting considerable interests because of their potential applications in solid oxide fuel cells (SOFC), oxygen sensors and oxygen-permeable membrane catalyst [1–4]. In this decade, a novel oxygen ion conductor $La_2Mo_2O_9$ (known as LAMOX) has been discovered [5] which has led to an interest in this new family of fast oxide-ion conductors. $La_2Mo_2O_9$ is known to undergo a phase transition from low temperature monoclinic α-phase, to a cubic high temperature β-phase at 853 K associated with a sharp jump in oxide ion conductivity [6]. The cubic form is known to exhibit oxide ion conductivity slightly higher than that of yttria-stabilized zirconia (YSZ). The high conductivity of the cubic form can be explained using the lone pair substitution (LPS) concept [7]. Various partial substitutions have been attempted on either the La site or Mo site or simultaneously at La and Mo sites in order to stabilize the high temperature phase to room temperature [8–11].

In this paper, detailed investigation of phase transition has been carried out, with pure, single and double substituted LMO. It has been reported that among the alkaline earth cations Sr doped $La_2Mo_2O_9$ shows the maximum conductivity [10] whereas V^{5+} doping at Mo site gives relatively high ionic transport among others [11]. Hence Sr^{2+} and V^{5+} were selected as doping ions. In La–Sr–Mo-oxides, $La_{1.96}Sr_{0.04}Mo_2O_{9-\delta}$ and for the V-doped compound, $La_2Mo_{1.95}V_{0.05}O_{9-\delta}$ showed maximum conductivity [10, 11] hence these particular compositions were selected. The fourth compound was taken by simultaneous doping at La and Mo sites, $La_{1.96}Sr_{0.04}Mo_{1.95}V_{0.05}O_{9-\delta}$.

Differential thermal analysis (DTA) and thermo-dilatometry were performed to examine the phase transformation between room temperature and 900 K. The oxygen ion conduction properties were also investigated using impedance spectroscopy.

Experimental

$La_2Mo_2O_9$ (LMO) and its derivatives $La_{1.96}Sr_{0.04}Mo_2O_{9-\delta}$ (LSMO), $La_2Mo_{1.95}V_{0.05}O_{9-\delta}$ (LMVO) and $La_{1.96}Sr_{0.04}Mo_{1.95}V_{0.05}O_{9-\delta}$ (LSMVO) were prepared by ceramic route. The stoichiometric amounts of La_2O_3, MoO_3, V_2O_5 and $SrCO_3$ (each with purity of 99.9%) were used as starting materials. La_2O_3 was annealed in air at 1173 K for 10 h and MoO_3 at 673 K for 5 h to ensure that these oxides were free from absorbed species like moisture and CO_2. The homogeneous mixture (~2 g) was pelletized and heated at 823 K for 60 h in air with two intermittent grindings. The final calcination was carried out in air at 973 K for 10 h. Even though in earlier literature [10] these types of compounds were synthesized at 1173 and sintered at 1473 K, synthesis at temperature as low as 973 K has not been attempted. Since MoO_3 is low melting material (1068 K), and un-reacted MoO_3 will have high vapor pressures at that temperature the reaction was carried out at lower temperature (973 K) with longer reaction time. Similarly in case of vanadium containing compounds, along with MoO_3, V_2O_5 is also a low melting material with melting point 963 K, so preparation at low temperature (973 K) does not pose any kinetic problem.

* Author for correspondence: shyamala@barc.gov.in

1388–6150/$20.00

Akadémiai Kiadó, Budapest, Hungary
Springer, Dordrecht, The Netherlands

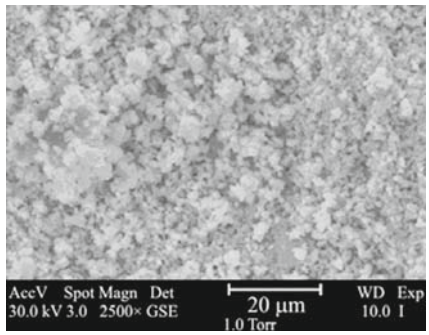

Fig. 1 SEM photograph of $La_2Mo_2O_9$

Room temperature X-ray powder diffraction patterns were recorded on a Philips diffractometer (PW 1729) with Ni filtered CuK_α radiation and using silicon as an external standard. The measurements were performed in the range of 10 to 70° in a continuous scan mode with a step width of 0.02° and at a scan rate of 0.5° min^{-1}. These patterns were indexed to generate their lattice dimensions using POWD program (version 2.2) [12]. High temperature X-ray powder diffraction patterns were recorded for pure $La_2Mo_2O_9$ on a Philips diffractometer (HTK-16, X'Pert Pro) with Ni filtered CuK_α radiation in the range of 20 to 70° in a continuous scan mode with a step width of 0.02° and at a scan rate of 0.5° min^{-1} at room temperature, 573, 773, 823, 873 and 973 K both in the heating and cooling cycles to see the evolution of phases with temperature.

Phase transition studies were carried out using a SETARAM simultaneous TG-DTA instrument (model 92-16.18). The thermal cycling was carried out for all the samples (~0.11 g) in argon flow as well as in air at 10 K min^{-1} from room temperature to 900 K and back. Thermo-dilatometric cycling was done in argon atmosphere using a thermo-mechanical analyzer (TMA, 92-12, SETARAM) in the temperature range of 300 to 973 K at the heating rate of 10 K min^{-1}. For dilatometric measurements the samples were pelletized (1.0 cm diameter) at a pressure of $4 \cdot 10^6$ g cm^{-2} and sintered at 973 K for 24 h.

Electrochemical characterization was done from AC impedance data of these samples recorded using Impedance/Gain-Phase Analyzer (Solartron 1260). The samples were made into pellets of 1.2 cm diameter and 0.5 cm thickness. Platinum paste (MaTeck GmbH, Germany) was applied on both sides of the pellets and cured at 773 K in air for 5 h. The packing density for the pellets was found to be ~63%, which was further, confirmed using scanning electron micrograph (Fig. 1). These pellets were used for impedance measurements in the range of 10 MHz to 0.1 Hz in air in the temperature range of 673–858 K.

Results and discussion

XRD patterns of LMO, LSMO, LMVO and LSMVO (calcined at 823 K for 60 h and final sintering at 973 K for 10 h) are shown in Fig. 2a. Major reflections in all the powder patterns were similar. LMO could be best indexed on the basis of monoclinic symmetry that matches with low temperature α-phase of $La_2Mo_2O_9$.The reflections of LSMO, LMVO and LSMVO could be indexed with cubic symmetry (Table 1) that matches with high temperature cubic phase of $La_2Mo_2O_9$ (JCPDF No. 28-0509). The reflections of $La_2Mo_2O_9$ at 573, 823 and 973 K were also indexed and tabulated in Table 2 along with the room temperature values. On substitution, the diffraction line (102) and (231) changed to (210) and (321), respectively. This is due to change in symmetry from monoclinic to cubic, where all the lattice parameter a, b and c, become equal and β changes from 90.36 to 90°. Similar kind of behavior is well reported with yttria stabilized zirconia, where high temperature cubic form is stabilized by doping Y_2O_3 in monoclinic ZrO_2 [13]. All the substituted samples showed lower cell volume as com-

Table 1 Cell parameters of LAMOX compounds

Compound	System	Unit cell parameters
LMO	monoclinic	a=7.152(2) Å, b=7.159(2) Å, c=7.163(1) Å, β=90.36(5)°, V=366.70(5) $Å^3$
LSMO	cubic	a=7.142(1) Å, V=364.27(2) $Å^3$
LMVO	cubic	a=7.142(1) Å, V=364.29(2) $Å^3$
LSMVO	cubic	a=7.145(3) Å, V=364.81(5) $Å^3$

Table 2 Cell parameters of LMX as a function of temperature

System	Temperature/K	Unit cell parameters
Monoclinic	298	a=7.152(2) Å, b=7.159(2) Å, c=7.163(1) Å, β=90.36(5)°, V=366.70(5) $Å^3$
Monoclinic	573	a=7.175(6) Å, b=7.196(7) Å, c=7.203(15) Å, β=90.5(2)°, V=371.9(9) $Å^3$
Monoclinic	823	a=7.162(4) Å, b=7.203(3) Å, c=7.212(1) Å, β=90.4(1)°, V=372.1(3) $Å^3$
Cubic	973	a=7.240(2) Å, V=379.6(2) $Å^3$

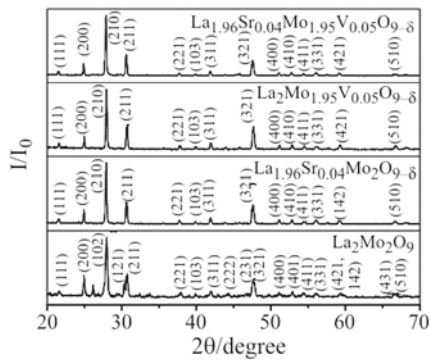

Fig. 2a XRD patterns of the α-$La_2Mo_2O_9$ along with its derivatives

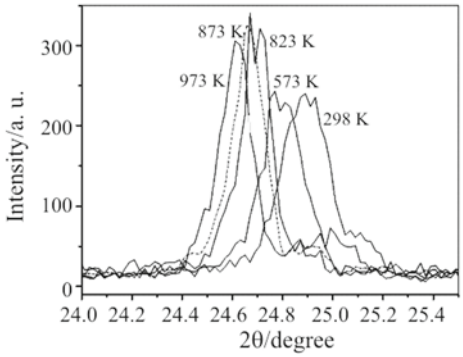

Fig. 2b Plot showing a magnified XRD peak of $La_2Mo_2O_9$ at room temperature and four other higher temperatures as obtained in the cooling cycle in HTXRD study

pared to LMO. Figure 2b shows an expanded view of a single reflection peak of $La_2Mo_2O_9$ at 973, 873, 823, 573 K and at room temperature during cooling. A change in the nature of splitting observed as the compound is cooled from 973 K to room temperature. The unit cell parameters shows discontinuity around 823 K compared to those determined above and below this temperature (Table 2) which indicates the existence of an intermediate transition around 823 K.

Figure 3 shows the DTA plots during heating and cooling in argon atmosphere, of low temperature α-$La_2Mo_2O_9$ in the temperature interval of 700–9000 K. α-$La_2Mo_2O_9$ transforms to high temperature β-phase at 842 K. In literature α→β phase transition of LMO in air occurs at 853 K [5] that is slightly higher than our value. This difference can be ascribed to different heating rate and atmosphere. It was found to be reversible with hysteresis of ~20 K. During cooling from 900 K, the exothermic peak shows a clear split. The split indicates that β-phase converts to an intermediate metastable phase (γ-phase), and then goes to α-phase. The reproducibility of the above DTA peaks during heating and cooling was established by recording DTA curves on four different samples of LMO. The split due to the formation of the metastable phase was obtained at the same temperature when the runs were taken in air. This is the first evidence of γ-$La_2Mo_2O_9$. This split is however not observed during cooling if the samples are sintered at a temperature of 1173 K indicating that β→α transition does not occur via the γ-phase. Neither is the split observed in the cooling cycle of DTA runs taken for the substituted compounds. This indicates that the metastable γ-phase is formed as a result of kinetic hindrance offered to the β→α conversion during cooling in pure LMO. Other substituted samples do not show the split, since substitution creates vacancies which facilitates β→α conversion kinetically and hence prevents the formation of the metastable γ-phase in substituted compounds. When pure LAMOX is heated to high temperature (1173 K) vacancies are created due to partial reduction Mo (6+) to Mo (5+) which again facilitates the cubic to monoclinic transition during cooling. So the metastable phase is observed only in low-temperature heated samples. The phase transition of all the above compounds was studied using DTA technique. DTA curves during heating, for all the samples with equal amount, are shown in Fig. 4. All the four samples clearly showed α→β transformation. The existence of the endothermic peak even after individual substitution of Sr^{2+}

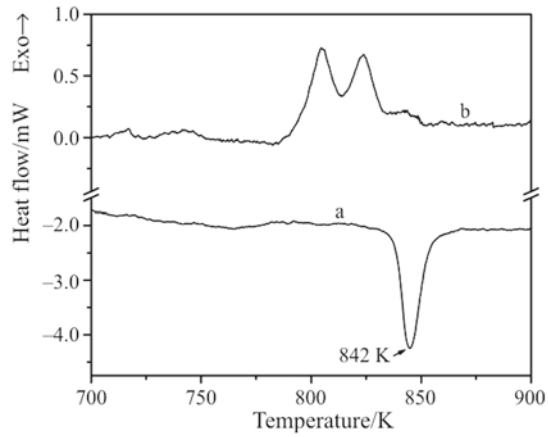

Fig. 3 DTA peak for $La_2Mo_2O_9$ during a – heating and b – cooling

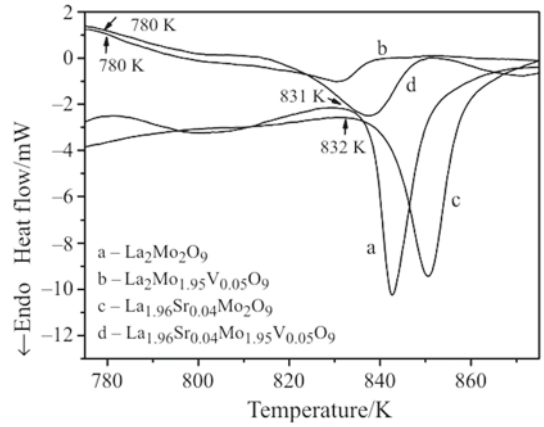

Fig. 4 DTA curves of LAMOX samples

and V^{5+} or simultaneous substitution of both Sr^{2+} and V^{5+} in LMO indicates that substitution could not suppress the phase transition completely in the above compounds. This clearly suggests that these low temperature synthesized samples can either have monoclinic symmetry (α-phase) or they are mixtures of α-phase and β-phase. The DTA curves of pure and Sr substituted LMO show sharp and strong endothermic peaks at 842 and 850 K, respectively. Vanadium substituted compounds like LMVO and LSMVO showed a considerable lowering of the phase transition temperature and also a lowering of enthalpy of transition. The lowering of the transition temperature and decrease in the enthalpy change corresponding to the transition can be due to incorporation of the larger V^{5+} ion in place of smaller Mo^{6+} site which induces structural distortion and thus lowers the transition temperature. But when Sr^{2+} is substituted in place of La^{3+} transition occurs at higher temperature indicating that the structural distortion is reduced. The lowering of enthalpy and temperature of transition might also be due to the fact that in $La_2Mo_2O_9$ Mo is tetrahedrally coordinated and the ionic radius of Mo (6+) is 0.41 Å whereas the ionic radius of V (5+) in the same environment is 0.36 Å. The ionic potential of hexavalent Mo is higher than that of pentavalent V which imparts more rigidity to the lattice having only Mo. This requires more energy and hence higher temperature for the transition to occur.

One cannot rule out completely the possibility of coexistence of both α- and β-phase in different concentration since XRD cannot separate these two phases, on account of the difference in the XRD patterns of the two phases being only a split in (211) and (231) lines for the α-phase which appear as shoulders to the main peaks. The dilatometric cycling for linear thermal expansion measurements were carried out on all the four samples using thermodilatometry in the temperature range of 300–1000 K. Thermal cycling for LMO and LSMO for linear expansion is shown in Figs 5a and b. A clear thermal hysteresis is seen in all the compounds indicating that it is a first order phase transition with structural rearrangements. During cooling cycle of LMO, a clear two-step curve is seen indicating that β→α conversion takes place via third phase that is stable over small range of temperature. It can be assumed that during cooling of the high temperature cubic β-phase two things happen: *i*) the averaging effect of lattice parameter (averaging of different 'a', 'b' and 'c' values of monoclinic lattice to a single 'a' value of the cubic lattice that occurs during heating) is reduced and *ii*) deformation of unit cell takes place that converts cubic phase to monoclinic α-phase and it requires small amount of energy. These two phenomena might be taking place in succession in case of LMO

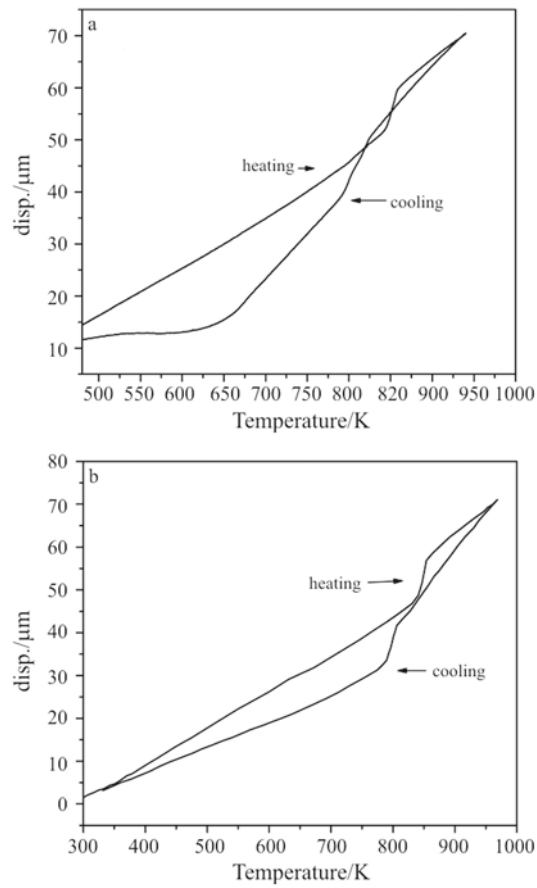

Fig. 5 Plot of average linear displacement *vs*. temperature during heating and cooling for a – $La_2Mo_2O_9$ and b – $La_{1.96}Sr_{0.04}Mo_2O_9$

whereas for the substituted compounds they happen simultaneously thereby avoiding the formation of the metastable phase. Thermal expansion curves during heating for all the samples are shown in Fig. 6. An obvious break in the thermal expansion curve from 780 to 840 K for all the samples was noticed which indicates that phase transition occurs in all the four samples and it supports our earlier DTA results. In all the cases thermal expansion coefficient of β-phase is higher as compared to α-phase (Table 3). The thermal expansion coefficient of LSMVO is similar to LMO in both the phases.

The Arrhenius plot of the electrical conductivity in the 600–850 K temperature range is shown in Fig. 7, for all the four compounds. The electrical conductivity increases with increase in temperature. As compared to LMO, the substituted derivatives showed higher conductivity in the α-phase and in lower temperature range (650–700 K) double substituted compound (LSMVO) showed highest conductivity. Earlier studies have shown that substitution at La^{3+} site or Mo^{6+} site can stabilize the high temperature cubic phase at room temperature [8–11, 14, 15], and in some cases with an increase in the ionic con-

Table 3 DTA peak temperature and TEC values of LAMOX samples

Composition	DTA peak/K	Temperature/K	$\alpha_{av.}\cdot 10^6/K^{-1}$
$La_2Mo_2O_9$	842	303–833 858–957	15.47 21.74
$La_2Mo_{1.95}V_{0.05}O_{9-\delta}$	831	303–783 838–958	16.05 26.65
$La_{1.96}Sr_{0.04}Mo_2O_{9-\delta}$	850	303–793 858–973	17.22 22.40
$La_{1.96}Sr_{0.04}Mo_{1.95}V_{0.05}O_{9-\delta}$	837	303–793 847–973	15.49 21.89

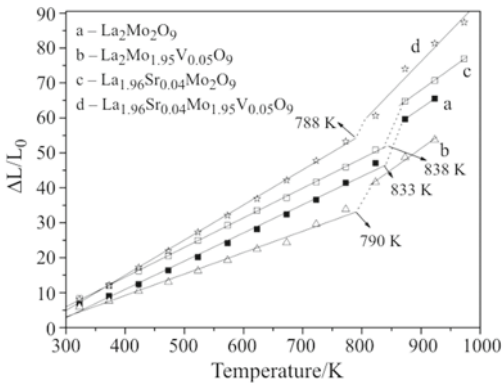

Fig. 6 Plot of average percentage linear thermal expansion *vs*. temperature of LAMOX samples

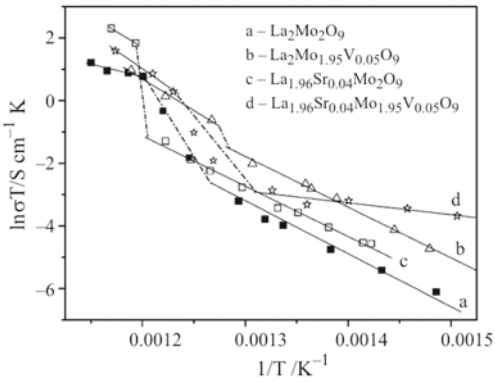

Fig. 7 Plot of lnσT *vs*. 1/*T* for LAMOX samples

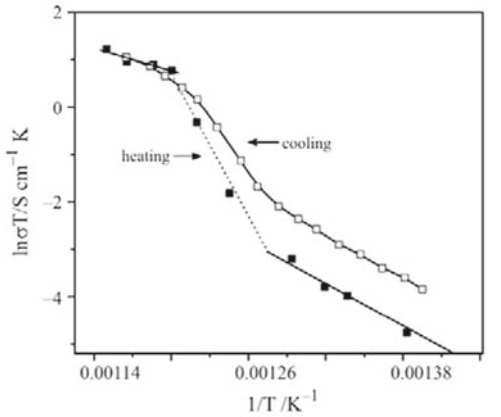

Fig. 8 Arrhenius plot of $La_2Mo_2O_9$ during heating and cooling

ductivity of $La_2Mo_2O_9$. A definite conclusion on the effect of substitution on β-$La_2Mo_2O_9$ is yet to be established. When V^{5+} ions are substituted for Mo^{6+} ions in the lattice β-phase stabilizes at room temperature but it also introduces extra oxygen vacancies (extrinsic defects) apart from the intrinsic vacancies already existing in $La_2Mo_2O_9$ that should increase the conductivity. In case of the doubly substituted compound even though the overall vacancy concentration is higher, a lower conductivity is observed which might be due to clustering of these vacancies [16].

The plot of ln(σT) *vs*. 1/*T* of α-$La_2Mo_2O_9$ during heating and cooling is shown in Fig. 8. In this case also temperature hysteresis during cooling could be seen which is indicative of the presence of a metastable γ-phase.

Conclusions

On reinvestigating the phase transition in low temperature sintered $La_2Mo_2O_9$ using DTA and dilatometry, it was observed that high temperature β-phase converts to low temperature α-phase through an intermediate metastable γ-phase. The formation of metastable phase was not seen in substituted compounds. The sudden jump in thermal expansion and ionic conductivity ~700 K supports first order phase transition in these compounds. The ionic conductivity values of the doubly-doped sample were least which could be due to clustering of the vacancies. The substitution increases ionic conductivity in α-phase of LMO, whereas in β-phase ionic conductivity reduces on substitution.

Acknowledgements

The authors sincerely thank their colleague Dr. S. N. Achary for the help rendered by him to delineate the crystal structures of the high temperature phases.

References

1 H. Yahiro, T. Ohuchi and K. Eguchi, J. Mater. Sci., 23 (1988) 1036.
2 N. Q. Minh, J. Am. Ceram. Soc., 76 (1993) 563.
3 K. Kakinuma, H. Yamamura and T. Atake, J. Therm. Anal. Cal., 69 (2002) 897.
4 L. F. Brum Malta and M. E. Medeiros, J. Therm. Anal. Cal., 81 (2005) 149.
5 P. Lacorre, Nature, 404 (2000) 856.
6 F. Goutenoire, O. Isnard, R. Retoux and P. Lacorre, Chem. Mater., 12 (2000) 2575.
7 P. Lacorre, Solid State Sci., 2 (2000) 755.
8 S. Basu, P. Sujatha Devi and H. S. Maiti, J. Electrochem. Soc., 152 (2005) A2143.
9 J. Yang, Z. Gu, Z. Wen and D. Yan, Solid State Ionics, 176 (2005) 523.
10 R. Subasri, D. Matusch, H. Nafe and F. Aldinger, J. Eur. Ceram. Soc., 24 (2004)129.
11 I. P. Marozau, D. Marrero-Lopez, A. L. Shaula and V. V. Kharton, Electrochim. Acta, 49 (2004) 3517.
12 E. Wu, POWD-an interactive Powder Diffraction Data Interpretation and indexing Program Version 2.2, Flinders University of South Autralia, 1988.
13 Fuel Cell Technologies: State and Perspectives, N. Sammes, A. Smirnova and O. Vasylyev, Eds, Nato Science Series Published by Springer, Netherlands 2005, P-23.
14 F. Goutenoire, O. Isnard, E. Suard, O. Bohnke, Y. Laligant, R. Retoux and P. Lacorre, J. Mater. Chem., 11 (2001) 119.
15 A. Arulraj, F. Goutenoire, M. Tabellout, O. Bohnke and P. Lacorre, Chem. Mater., 14 (2002) 2492.
16 T. L. Nguyen, M. Dokiya, S. Wang, H. Tagawa and T. Hashimoto, Solid State Ionics, 130 (2000) 229.

Received: October 1, 2008
Accepted: October 3, 2008
Online First: February 4, 2009

DOI: 10.1007/s10973-008-9532-y